The aromaticity and antiaromaticity of dehydroannulenes

Jonas Jusélius and Dage Sundholm

Department of Chemistry, P.O. Box 55 (A.I. Virtasen Aukio 1), FIN-00014 University of Helsinki, Finland. E-mail: jonas@iki.fi; sundholm@chem.helsinki.fi

The molecular structures and the magnetic properties of hexadehydro[12]annulenes and dodecadehydro[18]annulenes have been studied at *ab initio* and density-functional levels. The calculations show that the unsubstituted dehydro[12]annulene sustains a paratropic ring current in an external magnetic field, while the ring current for the unsubstituted dehydro[18]annulene is diatropic. Since the induced ring current is one measure of the molecular aromaticity, dehydro[18]annulene can be considered aromatic and dehydro[12]annulene antiaromatic. Fused benzene or cyclobutadiene rings destroy both the antiaromaticity and the aromaticity of the dehydroannulenes, while the substitution of the six hydrogens by ethinyl groups affects the aromatic properties of the dehydroannulenes only slightly. The calculations show that the bond alternation is smaller for molecules sustaining large diatropic or paratropic ring currents than for nonaromatic molecules. The ring-current contributions to the ^{1}H NMR chemical shieldings have been estimated for the molecules studied.

I. Introduction

Hexaethinylhexadehydrotribenzo[12]annulene (**1**) and hexaethinyldodecadehydrotribenzo[18]annulene (**6**) are the basic building units for graphyne and graphdiyne, respectively, which belong to a family of interesting and potentially important allotropes of carbon.[1–4] The graphyne and graphdiyne allotropes possess a remarkable planar network consisting of only benzene rings and alkyne units. The π-conjugation of graphyne and graphdiyne are expected to result in interesting magnetic[5,6] and nonlinear optical molecular properties.[3,4,7] Graphyne and graphdiyne have never been synthesized. Instead, the natural strategy to study them experimentally has been to synthesize different oligomers of (**1**) and (**6**) and to investigate their properties, which are then extrapolated to the infinite graphyne and graphdiyne networks.[3]

The dodecadehydro[18]annulene rings (**6–10**) possess 18 π-electrons which, according to the Hückel $(4n + 2)\pi$ rule, suggests that they are aromatic. The hexadehydro[12]annulene rings (**1–5**), on the other hand, have 12 π-electrons and they should therefore be antiaromatic. In an external magnetic field, aromatic molecules sustain an induced diatropic (diamagnetic) ring current, while for antiaromatic molecules the current circulates in the opposite direction *i.e.* they sustain a paratropic (paramagnetic) current.[5,8–12] The induced ring current creates a magnetic field which is observed as a long-range magnetic shielding. The short-range contribution to the magnetic shielding function due to the local motion of the electrons around the atoms and in the chemical bonds vanishes outside the electron density. This implies that the strength of the ring current of aromatic and antiaromatic molecules can be estimated by studying the long-range magnetic shielding function.[13–15] One measure of the degree of aromaticity is the strength of the induced ring current. Molecules sustaining a ring current in a magnetic field are not necessarily aromatic or antiaromatic, but molecules with neither induced diatropic nor paratropic ring currents are unlikely to be aromatic or antiaromatic.

The aim of this work is to study the magnetic properties of dehydroannulenes computationally. The molecular structures of hexaethinylhexadehydrotribenzo[12]annulene (**1**), hexadehydrotribenzo[12]annulene (**2**), hexadehydrohexaethinyl[12]annulene (**3**) hexadehydro[12]annulene (**4**), hexadehydrotricyclobutadien[12]annulene (**5**), hexaethinyldodecadehydrotribenzo[18]annulene (**6**), dodecadehydrotribenzo[18]annulene (**7**), dodecadehydrohexaethinyl[18]annulene (**8**), dodecadehydro[18]annulene (**9**) and dodecadehydrotricyclobutadien[18]annulene (**10**) have been obtained at the density-functional level of theory, while the nuclear magnetic shieldings and the induced ring currents, which are related to the degree of the aromaticity, have been studied at the Hartree–Fock level.

II. Computational methods

The molecular structures have been optimized at the resolution-of-the-identity density-functional theory (RI-DFT) level[16] using the Becke–Perdew (B–P) parametrization[17–19] as implemented in TURBOMOLE.[20] The nuclear magnetic shieldings have been calculated at the Hartree–Fock self-consistent field (SCF) level[21] using London or gauge-including-atomic orbitals (GIAO).[10,22]

In the structure optimization, the Karlsruhe split-valence basis sets[23] augmented with polarization functions on C were employed (SV(P)), while in the subsequent shielding calculations, the basis set was further augmented with polarization functions on H (SVP).

In the aromatic ring-current shieldings (ARCS) method,[13–15] the magnetic shieldings are calculated at selected point along a line perpendicular to the molecular plane starting at the center of the molecule. By considering the molecular ring as an infinitely thin wire carrying a current, a simple relation between the long-range behavior of the isotropic nuclear magnetic shielding function, and the current susceptibility with respect to the applied magnetic field can be derived[13–15] using Biot–Savart's law.[24] To check the electron-correlation effects, the molecular structure, the NMR shieldings, and the ARCS values were also calculated for (**4**) at the second-order Møller-Plesset (MP2) level[25–27] using the SVP

basis sets. The basis-set dependence was checked by performing calculations using triple-zeta quality basis sets augmented with polarization functions (TZVP).[28]

III. Results and discussions

The carbon–carbon distances for the dehydroannulenes obtained at the B–P DFT level are given in Table 1. The bond labels are defined in Fig. 1 and 2.

As seen in Table 1, all studied molecules have alternating bond lengths. The bond-length alternation for (3), (4), (8) and (9) is smaller than for (1), (2), (5), (6), (7) and (10). The R_3 bond in (5) and (10), which is formally a single bond, is only 134 pm, while for the other molecules it is 139–143 pm. For comparison, the bond length of a typical carbon–carbon single bond obtained at the B–P DFT level is 153 pm. A double bond is typically 134 pm, and a triple bond is 122 pm. The C–C distance obtained at the B–P DFT level for benzene is 140.6 pm and for 2-butyne the length of the formal single bond is 137 pm.
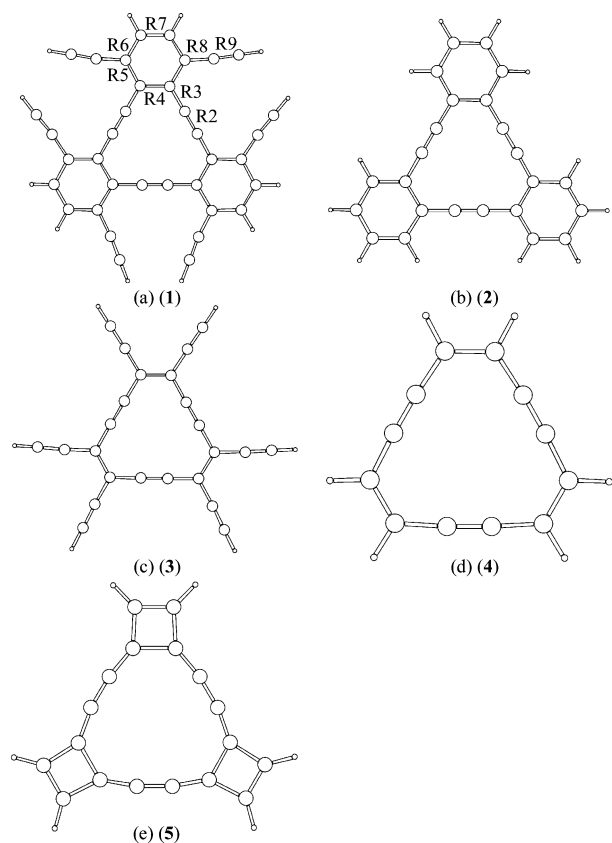

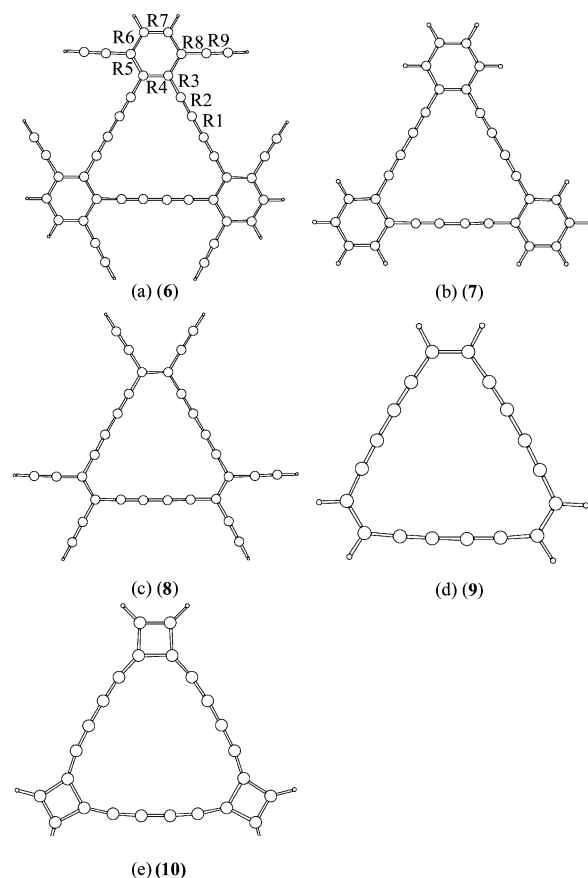Fig. 1 The molecular structures of the dehydro[12]annulenes (1), (2), (3), (4) and (5).

Fig. 2 The molecular structures of the dehydro[18]annulenes (6), (7), (8), (9) and (10).

The bond lengths of (1), (2), (6) and (7) are very similar even though (1) and (2) according to the Hückel rule are expected to be antiaromatic, while (6) and (7) should be aromatic. This observation suggests that these molecules have the same aromatic properties *i.e.* most likely they are nonaromatic.

For (5) and (10), the common bond of the fused cyclobutadiene ring and the annulene ring is 153 pm and must be considered to be a single bond. As seen in Table 1, for (5) and (10), the other bond distances of the annulene rings are significantly shorter (about 130 pm) with a relatively small bond-length alternation. This means that the bond conjugation of the tricyclobutadieneannulenes differs from the rest of the molecules studied. The three cyclobutadiene rings are connected by cumulative double bonds yielding an allene structure.

The molecular structures for (4) calculated at the MP2 and the B–P DFT levels are very similar. At the MP2 level, the C–H distance is 109.4 pm or 1.1 pm shorter than obtained in the B–P DFT optimization. The R_2, R_3 and R_4 bond dis-

Table 1 The carbon–carbon distances[a] (in pm) for the studied molecules calculated at the B–P DFT level using SV(P) basis sets

Molecule	R_1	R_2	R_3	R_4	R_5	R_6	R_7	R_8	R_9
(1)		123.4	142.2	144.2	143.3	141.9	139.1	142.6	122.6
(2)		123.3	142.4	144.1	141.7	140.2	140.7		
(3)		123.3	142.3	141.0				142.4	122.7
(4)		123.4	142.0	137.5					
(5)	127.5	133.9	152.6	147.6	138.9				
(6)	135.4	124.2	141.2	144.2	143.7	141.5	139.8	142.7	122.6
(7)	135.6	124.2	141.5	144.5	142.1	139.8	141.1		
(8)	134.2	125.0	139.7	143.5				142.6	122.7
(9)	134.1	125.2	138.7	140.2					
(10)	130.8	128.0	133.7	153.3	147.5	138.9			

[a] For the numbering of the bonds, see Fig. 1 and 2.

tances obtained at the MP2 level are 123.7, 142.3 and 136.6 pm, respectively, as compared to the B–P DFT bond distances of 123.4, 142.0 and 137.5 pm. The bond angles obtained at the MP2 and the DFT levels agree within 1°. The optimized molecular structures are available on our world-wide-web (www) server.[29]

The current susceptibilities and the ring-current radii have been deduced from the long-range shielding function as previously described.[13–15] The geometrical radii, the ring-current radii, and the current susceptibilities obtained in the ARCS calculations are given in Table 2. The ARCS plots for the unsubstituted dehydroannulenes (4) and (9) are shown in Fig. 3. For (9), the magnetic shielding function, $\sigma(z)$, is positive, while for (4) it is negative. The long-range part of $\sigma(z)$ shows that there are indeed strong ring currents in these molecules. For (9), the ring current is diatropic, while for (4), the ARCS fit yielded a paratropic ring current whose strength is −6.17 nA when the strength of the external magnetic field is 1 T. The current susceptibility for (4) can be compared to the current susceptibility of 8.0 nA T^{-1} for the benzene molecule.

The ethinyl groups reduce the aromatic and antiaromatic character of the annulene rings only slightly. The current susceptibilities for the hexaethinylannulenes (3) and (8) are about 20% smaller than for the corresponding unsubstituted dehydroannulenes (4) and (9). Since ring current is one measure of the molecular aromaticity, one can argue that (8) and (9) are aromatic, while (3) and (4) can be considered antiaromatic. For (1), (2), (5), (6), (7) and (10), the current susceptibilities are very small which indicates that they are nonaromatic.

For (8) and (9), which have large diatropic ring currents, the R_3 bond is shorter than for the nonaromatic molecules and the antiaromatic (3) and (4). For the antiaromatic (3) and (4), the R_4 bond is shorter than for the aromatic and the nonaromatic dehydroannulenes. The bond alternation is larger for the nonaromatic molecules than for the molecules sustaining large diatropic or paratropic ring currents.

The fused aromatic benzene rings reduce the diatropic and the paratropic currents of the [18]annulene and the [12]annulene rings, respectively. For (1) and (2), it is energetically more favorable to move π-electrons from the antiaromatic [12]annulene ring to the aromatic benzene rings making the benzene rings slightly less aromatic and the [12]annulene ring nonaromatic. For tribenzo[18]annulene, it is, as for molecules with fused aromatic rings in general, a conflict situation for the current directions.[6] The induced currents of the aromatic [18]annulene and of the aromatic

Table 2 The total energies (in E_h), the geometrical ring radius (in pm), the effective radius of the ring current (in pm), the induced ring-current susceptibility (in nA T^{-1}) obtained for the molecules studied

Molecule	Energy	Geometric radius	Current radius	$\dfrac{\partial I_{ring}}{\partial B_{ext}}$
(1)	−1377.534 253	248–264		
(2)	−920.994 922	249–264		
(3)	−916.884 426	247–262	203	−4.89
(4)	−460.337 606	249–260	197	−6.17[a]
(5)	−688.647 433	257–262	268	0.28
(6)	−1605.875 760	351–387	435	0.39
(7)	−1149.328 297	352–387	443	0.40
(8)	−1145.231 636	351–385	359	2.84
(9)	−688.693 557	355–383	367	3.30
(10)	−916.976 647	368–386	303	0.31
Benzene		134–141	122	8.00

[a] At the MP2 level the obtained current susceptibility ($\partial I_{ring}/\partial B_{ext}$) is −6.16 nA T^{-1} and the current radius is 197 pm.

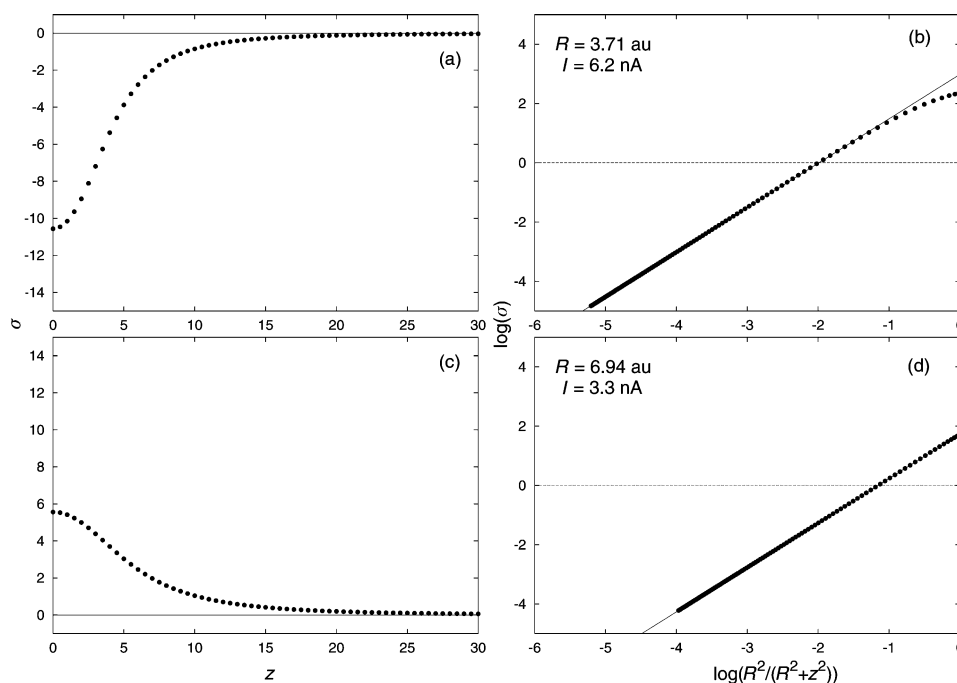**Fig. 3** The ARCS plots for the antiaromatic (4) and the aromatic (9) dehydroannulenes. (a) $\sigma(z)$ for dehydro[12]annulene (4); (b) ARCS fit for dehydro[12]annulene (4); (c) $\sigma(z)$ for dehydro[18]annulene (9); (d) ARCS fit for dehydro[18]annulene (9).

benzene rings meet from different directions at the common bond. This cancellation of the currents has serious consequences for the overall current pathway. The nuclear independent chemical shift (NICS)[30] values, given in Table 3, also indicate that the benzene rings remain almost as aromatic as for the free benzene molecule, while the [18]annulene ring becomes practically nonaromatic. For the tricyclobutadiene-annulenes (5) and (10), the common bond becomes a formal single bond and the conjugated but nonaromatic path includes the cyclobutadiene rings.

For the antiaromatic and aromatic dehydroannulenes, the obtained current radii are smaller than the geometrical radii. For the nonaromatic molecules (6) and (7), the obtained current radii are significantly larger than the geometrical radii, which reveal problems in the ARCS fit. For (1) and (2), the ARCS fits did not manage to give reliable values for the current susceptibilities and the current radii. Due to the absence of the long-range shieldings, the obtained current susceptibilities for the nonaromatic molecules are very small and inaccurate. The ARCS plots are also available on our www server.[29]

The NICS values in Table 3 support the conclusions drawn from the ring-current susceptibilities obtained in the ARCS calculations. Note that the present definition for the NICS values have the opposite sign as compared to the original definition by Schleyer et al.[30] The NICS values can be used as a relative measure of the aromaticity for closely related molecules. The NICS values do not, however, provide any accurate information about the strength of the ring current since the shielding at the center of the molecule depends on both the size of the circuit and the current strength. The small

negative NICS values for the cyclobutadiene in (5) and (10) indicate that the fused cyclobutadiene rings are antiaromatic. However, the common bond of the annulene and the cyclobutadiene rings is very long and hardly any current can pass it. The NICS values at the center of the annulene ring (see Table 3) and the ARCS values in Table 2 show that (5) and (10) are neither aromatic nor antiaromatic.

The total energies obtained at the B–P DFT level are given in Table 2. A comparison of the energies shows that the energy difference between the (9) and (4) analogs is 14 kcal mol^{-1} larger than the energy difference between the non-aromatic (7) and (2). The energy difference of 14 kcal mol^{-1} is an estimate for the difference between the aromatic and anti-aromatic (de)stabilization energies. The energy difference between (8) and (3) is, as their ring currents, smaller than for (9) and (4) yielding a difference in the aromatic and anti-aromatic (de)stabilization energies of about 9 kcal mol^{-1}. The energy difference between (6) and (1) is smaller since the ethinyl hydrogens in (1) are too close and introduce additional molecular strain. The molecular strain in (5) is larger than for (10) resulting in the smallest energy difference between the analogs.

There is a good agreement between calculated and measured chemical shifts. In Table 4, the ^{1}H NMR shieldings calculated at the Hartee–Fock level are compared to available experimental data. The small discrepancies between the calculated and measured NMR shifts are due to rovibrational corrections, electron correlation effects and basis-set truncation errors. The ^{1}H NMR shieldings for (4) calculated at the MP2 level show that the net electron correlation effects on the ^{1}H NMR chemical shift are about 1 ppm for the present molecules.

As seen in Table 5, the electron correlation contribution to the ^{1}H NMR shieldings for (4) is about $+0.8$ ppm, while for tetramethylsilane (TMS) it is -0.4 ppm. The ^{1}H NMR shieldings for (4) obtained using the DFT and the MP2 structures are practically equal, while for TMS the ^{1}H NMR shieldings obtained using the MP2 structure are about 0.4 ppm larger than with the DFT structure. The basis-set truncation errors were estimated by increasing the basis sets from SVP to TZVP. For (4), the ^{1}H NMR shieldings obtained with the TZVP basis sets are 0.13 ppm smaller than with the SVP basis sets. For TMS, the obtained basis-set effect is 0.10 ppm yielding a total basis-set correction of 0.23 ppm for the ^{1}H NMR chemical shift of (4). The extrapolated value for the ^{1}H NMR chemical shift is 3.55 ppm as compared to the experimental value of 4.42 ppm. The extrapolated ^{1}H NMR shifts and shieldings in Table 5 are obtained by adding the basis-set

Table 3 The NICS values calculated at the center of the [12]annulene and the [18]annulene rings as well as the NICS values of the fused benzene and cyclobutadiene rings (in ppm)

Molecule	Center	Fused rings
(1)	-2.89	9.30
(2)	-2.94	9.24
(3)	-8.82	
(4)	-10.56	
(5)	0.83	-2.98
(6)	-0.02	10.52
(7)	-0.07	10.55
(8)	4.85	
(9)	5.57	
(10)	0.42	-4.14
Benzene	10.68	10.68

Table 4 The calculated ^{1}H NMR chemical shifts relative to TMS ($\delta = \sigma_{\text{ref}} - \sigma$, in ppm) for the studied molecules as compared to experimental values. The estimated ring-current contributions ($\Delta\delta_{\text{RC}}$) to the ^{1}H NMR chemical shifts (in ppm) are also given

Molecule	$\delta(\text{H}^a)$(Calc.)	$\Delta\delta_{\text{RC}}$	$\delta(\text{H}^a)$(Exp.)	$\delta(\text{H}^b)$(Calc.)	$\Delta\delta_{\text{RC}}$	$\delta(\text{H}^b)$(Exp.)
(1)	7.32	-2.84	7.33^c	3.61	-0.72	3.32^c
(2)	7.28	-2.80	7.33^d	6.98	-2.80	7.18^d
(3)				3.99	0.26	
(4)	4.11	1.75	4.42^e			
(5)	6.96	~ 0				
(6)	7.45	-3.20		4.02	-0.80	
(7)	7.70	-3.20	7.68	7.24	-3.20	7.42
(8)				4.71	-0.30	
(9)	7.24	-1.87	7.02^f			
(10)	7.66	~ 0				
Benzene	7.18	-3.20	7.26^g			
Ethyne	1.14		1.48^g			
Ethene	5.41		5.31^g			
Ethane	0.86		0.88^g			

^{a} For the molecules with non-identical hydrogens, H^a denotes the hydrogen closer to the [12]annulene or the [18]annulene ring. ^{b} H^b denotes either the other hydrogen at the benzene ring or the ethinyl hydrogen. ^{c} Ref. 2. ^{d} Ref. 33. ^{e} Ref. 5 and 34. ^{f} Ref. 34. ^{g} See ref. 35 and references therein.

Table 5 The ^{1}H NMR shieldings (in ppm) for (**4**) and for TMS calculated at the SCF and the MP2 levels using the DFT and MP2 molecular structures. The corresponding ^{1}H NMR chemical shifts (in ppm) with respect to TMS are compared to the experimental value

Molecule	SCF(DFT)[a]	MP2(DFT)[a]	SCF(MP2)[a]	MP2(MP2)[a]	SCF(MP2)[b]	Extrapolated
(**4**)	27.35	28.26	27.42	28.22	27.29	28.09
TMS	31.46	31.12	31.89	31.54	31.99	31.64
$\delta_{Calc.}$	4.11	2.86	4.47	3.32	4.70	3.55
$\delta_{Exp.}$						4.42

[a] Using the SVP basis sets. [b] Using the TZVP basis sets.

corrections (SCF(MP2,TZVP)-SCF(MP2,SVP)) to the MP2(MP2,SVP) results. Since the electron-correlation contribution obtained at the MP2 level is rather small, it is unlikely that higher-order electron-correlation contributions would be of importance. The main reason for the remaining discrepancy of 0.87 ppm is the rovibrational corrections. The rovibrational effects on the ^{1}H NMR chemical shieldings are usually less than 1 ppm.[31] However, in some extreme cases they may be even larger than 1 ppm.[32]

The induced ring currents in the aromatic and the anti-aromatic annulene rings create a magnetic field which is observed as an additional contribution to the nuclear magnetic shieldings. The size of this current-induced magnetic shielding can be estimated by assuming that the wire carrying the current is circular and infinitely thin.[13,24] The ring-current contributions ($\Delta\delta_{RC}$) to the ^{1}H NMR chemical shifts are given in Table 4 and the ring radii are given in Table 2.

For benzene, the hydrogens lie 251 pm from the ring center. The ring-current susceptibility and the current radius obtained in the ARCS calculation are 8.0 nA T^{-1} and 122 pm, respectively, resulting in a ring-current shift of -3.2 ppm which, at first glance, seems to be too large. However, the difference in the ^{1}H NMR shifts for ethene and benzene of -1.95 ppm is not only due to the ring current. The bond order in ethene and benzene also differs and these two contributions to some extent cancel.

For the antiaromatic (**3**) and (**4**), the ring-current shifts originating from the current in the annulene rings are 0.26 and 1.75 ppm, respectively. The ring-current shift is significantly smaller for (**3**) since the hydrogens lie 789 pm from the molecular center. For the aromatic dehydroannulenes, the ring-current shifts are -0.30 and -1.87 pm, for (**8**) and (**9**), respectively. The fused benzene rings in (**1**), (**2**), (**6**) and (**7**) also sustain ring currents which shift the ^{1}H NMR signals. The ring-current strengths for the fused benzene rings are estimated from the NICS values given in Table 3.

IV. Summary

One measure of the aromaticity is the ring current induced by an external magnetic field. In this work, we have calculated the nuclear magnetic shielding function at selected points outside the molecules. The ring-current susceptibilities, which yield the induced ring current for a given field strength, have been deduced from the long-range behavior of the magnetic shielding function. The calculations show that the unsubstituted dehydro[12]annulene is antiaromatic, while the dehydro[18]annulene is aromatic. The fused cyclobutadiene and benzene rings destroy the aromaticity and the anti-aromaticity of the dehydroannulenes. The substitution of the ethinyl groups affects the aromatic and antiaromatic properties only slightly.

References

1 M. M. Haley, S. C. Brand and J. J. Pak, *Angew. Chem. Int. Ed. Engl.*, 1997, **36**, 836.
2 C. Eickmeier, H. Junga, A. J. Matzger, F. Scherhag, M. Shim and K. P. Vollhardt, *Angew. Chem. Int. Ed. Engl.*, 1997, **36**, 2103.
3 W. B. Wan, S. C. Brand, J. J. Pak and M. M. Haley, *Chem. Eur. J.*, 2000, **6**, 2044.
4 F. Diederich and Y. Rubin, *Angew. Chem. Int. Ed. Engl.*, 1992, **104**, 1123.
5 J. A. Pople and K. G. Untch, *J. Am. Chem. Soc.*, 1966, **88**, 4811.
6 P. Lazzeretti, *Prog. Nucl. Magn. Res. Spectrosc.*, 2000, **36**, 1.
7 R. H. Baughman, H. Eckhardt and M. Kertesz, *J. Chem. Phys.*, 1987, **87**, 6687.
8 L. Pauling, *J. Chem. Phys.*, 1936, **4**, 637.
9 K. Lonsdale, *Proc. R. Soc. London, Ser. A*, 1937, **159**, 149.
10 F. London, *J. Phys. Radium*, 1937, **8**, 397.
11 K. B. Wiberg, *Chem. Rev.*, 2001, **101**, 1317.
12 R. H. Mitchell, *Chem. Rev.*, 2001, **101**, 1301.
13 J. Jusélius and D. Sundholm, *Phys. Chem. Chem. Phys.*, 1999, **1**, 3429.
14 J. Jusélius and D. Sundholm, *Phys. Chem. Chem. Phys.*, 2000, **2**, 2145.
15 J. Jusélius and D. Sundholm, *J. Org. Chem.*, 2000, **65**, 5233.
16 K. Eichkorn, O. Treutler, H. Öhm, M. Häser and R. Ahlrichs, *Chem. Phys. Lett.*, 1995, **240**, 283.
17 S. H. Vosko, L. Wilk and M. Nusair, *Can. J. Phys.*, 1980, **58**, 1200.
18 J. P. Perdew, *Phys. Rev. B*, 1986, **33**, 8822.
19 A. D. Becke, *Phys. Rev. B*, 1988, **38**, 3098.
20 R. Ahlrichs, M. Bär, M. Häser, H. Horn and C. Kölmel, *Chem. Phys. Lett.*, 1989, **162**, 165.
21 M. Häser, R. Ahlrichs, H. P. Baron, P. Weis and H. Horn, *Theor. Chim. Acta*, 1992, **83**, 551.
22 K. Wolinski, J. F. Hinton and P. Pulay, *J. Am. Chem. Soc.*, 1990, **112**, 8251.
23 A. Schäfer, H. Horn and R. Ahlrichs, *J. Chem. Phys.*, 1992, **97**, 2571.
24 G. Arfken, *Mathematical Methods for Physicists*, Academic Press, Orlando, 1985.
25 F. Weigend and M. Häser, *Theor. Chem. Acc.*, 1997, **97**, 331.
26 M. Kollwitz and J. Gauss, *Chem. Phys. Lett.*, 1996, **260**, 639.
27 M. Kollwitz, M. Häser and J. Gauss, *J. Chem. Phys.*, 1998, **108**, 8295.
28 A. Schäfer, C. Huber and R. Ahlrichs, *J. Chem. Phys.*, 1994, **100**, 5829.
29 http://www.chem.helsinki.fi/~sundholm/qc/antiaromatic
30 P. von Rague Schleyer, C. Maerker, A. Dransfeld, H. Jiao and N. J. R. van Eikema Hommes, *J. Am. Chem. Soc.*, 1996, **118**, 6317.
31 D. Sundholm, J. Gauss and A. Schäfer, *J. Chem. Phys.*, 1996, **105**, 11051.
32 K. Ruud, P.-O. Åstrand and P. R. Taylor, *J. Am. Chem. Soc.*, 2001, in press.
33 A. J. Matzger and K. P. C. Vollhardt, *Tetrahedron Lett.*, 1998, 6791.
34 W. H. Okamura and F. Sondheimer, *J. Am. Chem. Soc.*, 1967, **89**, 5991.
35 W. Kutzelnigg, U. Fleischer and M. Schindler, *NMR Basic Principles and Progress*, Springer, Berlin, 1990, vol. 23, pp. 165–262.